Available online at www.sciencedirect.com
SCIENCE DIRECT®
Journal of Solid State Chemistry 174 (2003) 159–164
JOURNAL OF SOLID STATE CHEMISTRY
http://elsevier.com/locate/jssc

# Specific heat and neutron diffraction study on quaternary sulfides $BaNd_2CoS_5$ and $BaNd_2ZnS_5$

Makoto Wakeshima,[a,*] Nobuyuki Taira,[a] Yukio Hinatsu,[a] Aya Tobo,[b] Kenji Ohoyama,[b] and Yasuo Yamaguchi[b]

[a] *Division of Chemistry, Graduate School of Science, Kita 10-Nishi8, Kitaku Hokkaido University, Hokkaido University, Sapporo 060-0810, Japan*
[b] *Institute of Materials Research, Tohoku University, Sendai 980-8577, Japan*

Received 12 February 2003; accepted 31 March 2003

**Abstract**

Magnetic and electrical properties are investigated for quaternary neodymium sulfides $BaNd_2TS_5$ ($T$=Co, Zn) through the specific heat, neutron diffraction, and electrical conductivity measurements. Their electrical conductivities show semiconductive behavior, which follows the Arrhenius temperature dependence with the activation energy of $E_a = 1.46$ eV for $BaNd_2ZnS_5$ and $E_a = 1.19$ eV for $BaNd_2CoS_5$. The specific heat of $BaNd_2ZnS_5$ has a $\lambda$-type anomaly at 2.8 K due to the antiferromagnetic ordering of the $Nd^{3+}$ moments and a Schottky-type anomaly at around 60 K, which results from the crystal field splitting of the $^4I_{9/2}$ ground state of the $Nd^{3+}$ ion. The specific heat of $BaNd_2CoS_5$ shows two $\lambda$-type anomalies at 5.7 K due to the antiferromagnetic ordering of $Nd^{3+}$ and at 58 K due to the antiferromagnetic ordering of $Co^{2+}$. The latter overlaps with the Schottky-type anomaly due to the crystal field splitting of the $Nd^{3+}$ ion. Neutron diffraction measurements for $BaNd_2CoS_5$ show that a magnetic arrangement of the $Co^{2+}$ moments has a collinear antiferromagnetic structure, while that of the $Nd^{3+}$ moments has a noncollinear one.


*Keywords:* Specific heat; Neutron diffraction; Quaternary sulfide; Antiferromagnetic transition; Magnetic structure

## 1. Introduction

Many binary and ternary compounds containing rare earth and chalcogen have been synthesized [1,2]. These compounds adopt a wide range of structure types and show a variety of interesting physical properties [3]. However, studies on quaternary rare-earth chalcogenides are still scarce, compared with the case for binary and ternary compounds [4–9].

A series of quaternary transition metal sulfides $BaLn_2TS_5$ ($Ln$=lanthanides, $T$=Mn, Fe, Co, Zn) crystallizes in a tetragonal structure with the space group, $I4/mcm$ [10–13]. In these sulfides, the transition metal ions are bonded to four sulfur ions in a distorted tetrahedral coordination form and these $TS_4$ tetrahedra link via the Ba ions. The $Ln$ ion is bonded to eight sulfur neighbors with the $D_{2h}$ site symmetry [11]. Fig. 1 shows the schematic structure of $BaLn_2TS_5$.

Through the magnetic susceptibility measurements of $BaLn_2TS_5$, the Mn, Co, and Fe ions were found to be in the divalent state and were observed to occur an antiferromagnetic transition at ~60 K for Mn, at ~60 K for Co, and at ~40 K for Fe [11,12,14]. The powder neutron diffraction data of $BaLa_2TS_5$ ($T$=Mn and Co) indicated that the $Mn^{2+}$ and $Co^{2+}$ moments had a collinear antiferromagnetic structure at 10 K [15,16]. In the paramagnetic temperature region, the effective magnetic moments of the $Ln$ ions in the $BaLn_2TS_5$ were in good agreement with the theoretical moments of the free $Ln^{3+}$ ions. In addition, with decreasing temperature the $Nd^{3+}$ ions also showed an antiferromagnetic ordering below 3–6 K in the Nd compounds [12,14]. It seems that the magnetic moments of the $Nd^{3+}$ ions and $T^{2+}$ ions order independently below each of the antiferromagnetic transition temperatures. This magnetic behavior is understandable from its crystal structure, i.e., the $BaTS_4$ layers and $LnS$ layers are perpendicular to the $c$-axis and they are stacked alternately.

*Corresponding author. Fax: +81-11-746-2557.
*E-mail address:* wake@sci.hokudai.ac.jp (M. Wakeshima).

0022-4596/03/$ - see front matter © 2003 Elsevier Science (USA). All rights reserved.
doi:10.1016/S0022-4596(03)00193-2

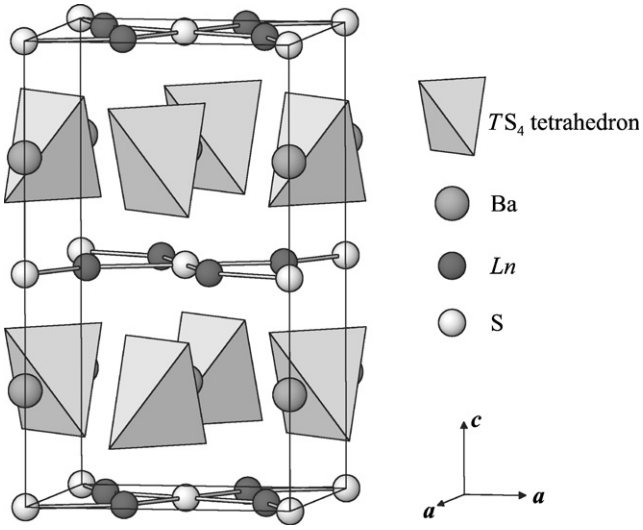


Fig. 1. Schematic crystal structure of $BaLn_2TS_5$.

In this study, we have paid our attention on two quaternary neodymium sulfides $BaNd_2MS_5$ ($T$=Co, Zn). Since the magnetic moments of two Nd ions greatly contribute to the magnetic susceptibilities of $BaNd_2CoS_5$, the antiferromagnetic ordering of $Co^{2+}$ ions were not clear in its magnetic susceptibilities vs temperature curve. So, we have determined the Néel temperature of the $Co^{2+}$ ions by calculating the first derivatives of the susceptibility against temperature [12].

In order to obtain additional experimental information and quantitative data on the magnetic ordering of $Co^{2+}$ and $Nd^{3+}$ ions, we have performed specific heat and neutron diffraction measurements on $BaNd_2CoS_5$ down to 1.8 K. Specific heat measurements have also been performed on $BaNd_2ZnS_5$ to estimate the magnetic entropy change due to only the antiferromagnetic ordering of the $Nd^{3+}$ ions. Furthermore, the electrical properties of both compounds have been investigated through electrical conductivity measurements.

## 2. Experimental

Quaternary neodymium sulfides $BaNd_2CoS_5$ and $BaNd_2ZnS_5$ were prepared by a solid-state reaction as described elsewhere [12]. The electrical conductivity of the sintered sample was measured by the DC four-probe method in the temperature range from 260 to 400 K. The specific heat was measured by a relaxation technique using a physical property measurement system (Quantum Design, PPMS) in the temperature range from 1.8 to 300 K. The sample in the form of pellet ($\sim$10 mg) was mounted on an aluminum plate with apiezon for better thermal contact.

Powder neutron diffraction measurements were carried out using the Kinken powder diffractometer for high-efficiency and high-resolution measurements, HERMES, of Institute for Material Research, Tohoku University, installed at the JRR-3M reactor in Japan Atomic Energy Research Institute, Tokai. Neutrons with wavelength of 1.8196 Å were obtained by the 331 reflection of the Ge monochromator and 12′-blank-22′ collimation [17]. The sample was set in a vanadium cylinder with a diameter of 10 mm and sealed in a standard aluminum cell with helium gas and was cooled down to low temperatures using a liquid helium cryostat. Intensity data from 3° to 140° were used in the crystal structure and magnetic structure refinements using Rietveld method program FullProf [18].

## 3. Results and discussion

### 3.1. Electrical conductivities

Fig. 2 shows the electrical conductivities ($\sigma$) of $BaNd_2ZnS_5$ and $BaNd_2CoS_5$ as a function of reciprocal temperature. Both the conductivities increase with temperature and follow the Arrhenius temperature dependence, $\sigma \propto \exp(-E_a/k_BT)$ with the activation energy of $E_a$. The activation energies were estimated to be 1.46 eV for $BaNd_2ZnS_5$ and 1.19 eV for $BaNd_2CoS_5$. The semiconductive behavior of these compounds indicate that the 4$f$ and 3$d$ electrons are localized on the Nd and Co ions, respectively, which is consistent with the result of their magnetic susceptibility measurements [12].

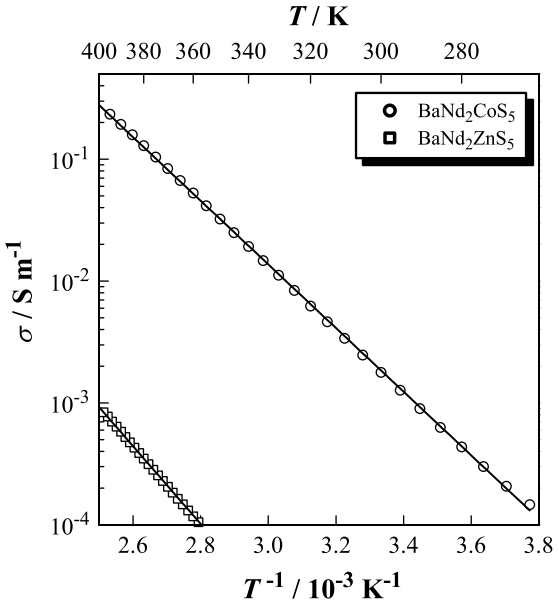


Fig. 2. Reciprocal temperature dependence of the electrical conductivity $\sigma$ of $BaNd_2TS_5$ ($T$=Co, Zn). Straight solid lines present the Arrhenius law fittings.

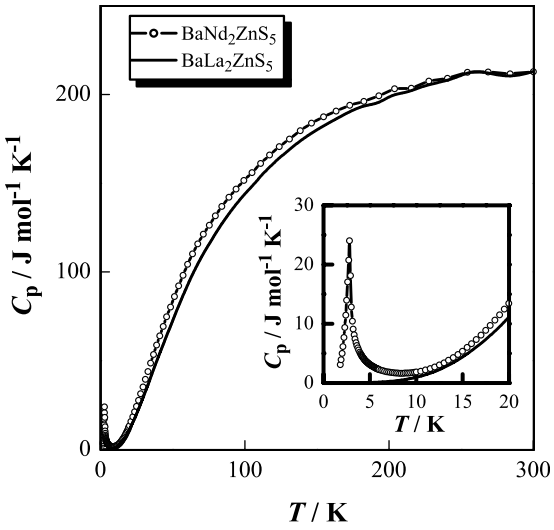


Fig. 3. Temperature dependence of the specific heat $C_p$ of $BaNd_2ZnS_5$ and $BaLa_2ZnS_5$ below 300 K. The inset shows $C_p$ below 20 K.

### 3.2. Specific heats

Fig. 3 shows the temperature dependence of the molar specific heats ($C_p$) of $BaNd_2ZnS_5$. A $\lambda$-type anomaly, which is attributable to an antiferromagnetic ordering of the $Nd^{3+}$ ions, is observed at 2.8 K as shown in the inset of Fig. 3. This experimental result is consistent with our magnetic susceptibility measurements [12]. The temperature dependence of the specific heats of a non-magnetic compound, $BaLa_2ZnS_5$, is also shown in Fig. 3. If we assume that the electronic and lattice contributions to the total $C_p$ are equal between $BaNd_2ZnS_5$ and $BaLa_2ZnS_5$, the magnetic specific heat ($C_{mag}$) of the $Nd^{3+}$ ions is obtained by subtracting the specific heat of $BaLa_2ZnS_5$ from that of $BaNd_2ZnS_5$. The temperature dependences of $C_{mag}$ and the magnetic entropy $S_{mag} = \int_0^T (C_{mag}/T)\,dT$ are shown in Fig. 4(a) and (b), respectively.

According to the antiferromagnetic spin-wave model, $C_{mag}$ for antiferromagnetic magnons is expected to be proportional to $T^3$ at $T < T_N$ ($\sim$2.8 K) [19]. The calculated values of $C_{mag}$ below 1.8 K are plotted as a broken line in Fig. 4(a). In the $C_{mag} - T$ curve, another broad peak appears at around 60 K except for the $\lambda$-type peak at 2.8 K. The $^4I_{9/2}$ ground state of the $Nd^{3+}$ ion should split into five Kramers' doublets by the crystalline electric field in the site symmetry of $D_{2h}$. In the antiferromagnetic state, only the lowest doublet needs to be considered, because

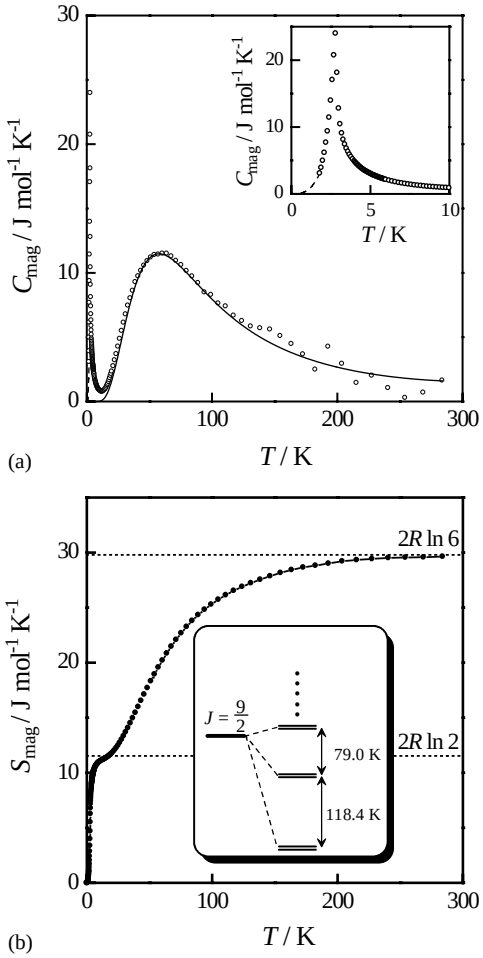


Fig. 4. (a) Temperature dependence of the magnetic specific heat $C_{mag}$ of $BaNd_2ZnS_5$. The inset shows $C_{mag}$ below 10 K. A broken line indicates the calculated $C_{mag}$ below $T_N$ (see text). The fitted curve (solid line) is the Schottky curve from the Nd energy levels (see text). (b) Temperature dependence of the magnetic entropy $S_{mag}$ of $BaNd_2ZnS_5$. The inset shows the crystal-field-splitting levels of the $Nd^{3+}$ ion in $BaNd_2ZnS_5$.

$S_{mag}$ converges at $2R\ln 2$ ($R\ln 2$ per mole of $Nd^{3+}$ ion) below 10 K, where $R$ is the gas constant. In addition, excited doublets contribute to the Schottky-type anomaly at around 60 K. Considering the energy levels with the energy $\varepsilon_0, \varepsilon_1, \ldots, \varepsilon_m$ of the degeneration $g_0, g_1, \ldots, g_m$, the partition function ($Z$) in this system is presented by $Z = \sum_{i=0}^{m} g_i \exp(-\varepsilon_i/kT)$ and the Schottky-type specific heat ($C_S$) is given by $C_s = \partial/\partial T(RT^2\,\partial \ln Z/\partial T)$. Therefore, for the $Nd^{3+}$ ion in $BaNd_2ZnS_5$, $C_S$ by four excited doublets is calculated by the following equation:

$$C_S = 2 \times \frac{\left[\sum_{i=1}^{4} \varepsilon_i^2 \exp(-\varepsilon_i/kT)\right] \times \left[1 + \sum_{i=1}^{4} \exp(-\varepsilon_i/kT)\right] - \left[\sum_{i=1}^{4} \varepsilon_i \exp(-\varepsilon_i/kT)\right]^2}{kT^2\left[1 + \sum_{i=1}^{4} \exp(-\varepsilon_i/kT)\right]^2}, \quad (1)$$

where $\varepsilon_i$ is the energy difference between the ground doublet and the $i$th excited doublet. By fitting Eq. (1) to the $C_{mag} - T$ curve as a solid line in Fig. 4(a), the first and second excited doublets were found to contribute mainly to the $C_S$ anomaly at around 60 K, and the energy differences from the ground-state doublet were estimated to be 118.4(4) K for the first excited doublet and 197.4(8) K for the second excited doublet. The value of $S_{mag} \sim 2R \ln 6$ at 300 K also indicates that the other two excited doublets scarcely affect the $C_S$ behavior at low temperatures.

Fig. 5(a) shows the temperature dependence of the molar $C_p$ of $BaNd_2CoS_5$. Two $\lambda$-type anomalies have been observed at corresponding temperatures with an antiferromagnetic ordering of the $Co^{2+}$ ions ($\sim$60 K) and that of $Nd^{3+}$ ions ($\sim$6 K) for their magnetic susceptibilities [3]. The temperature dependence of $C_{mag}$ for $BaNd_2CoS_5$ is obtained by subtracting the $C_p$ data of $BaLa_2ZnS_5$ from those of $BaNd_2CoS_5$ and is plotted in Fig. 5(b). The temperature dependence of $S_{mag}$ obtained by integrating the $C_{mag}/T$ data is also plotted in Fig. 5(b). For $BaNd_2CoS_5$, the coordination of the $Nd^{3+}$ ions which are bonded to eight sulfurs, was found

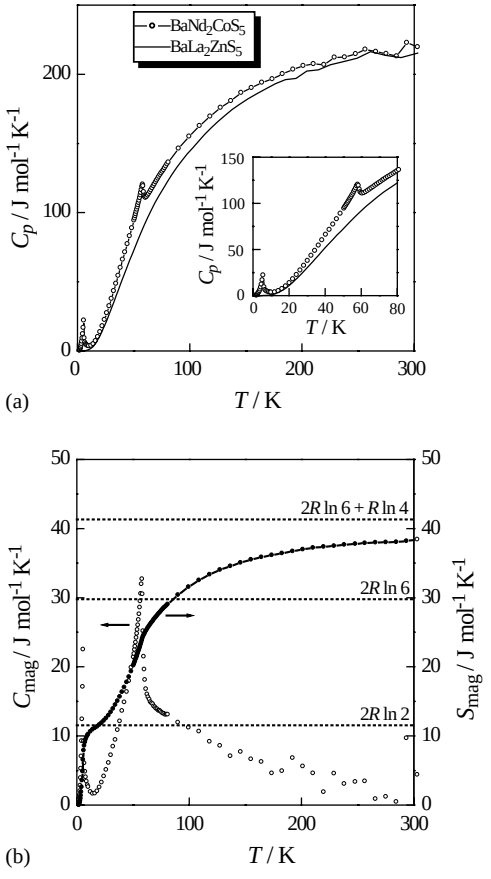


Fig. 5. (a) Temperature dependence of the specific heat $C_p$ of $BaNd_2CoS_5$ and $BaLa_2ZnS_5$ below 300 K. The inset shows $C_p$ below 80 K. (b) Temperature dependence of the magnetic specific heat $C_{mag}$ and the magnetic entropy $S_{mag}$ of $BaNd_2CoS_5$.

to be nearly the same as that for $BaNd_2ZnS_5$ through the powder X-ray diffraction measurements [12]. Thus, the crystal-field-splitting energy levels of the $^4I_{9/2}$ ground state of the $Nd^{3+}$ ions in $BaNd_2CoS_5$ are expected to be similar to those in $BaNd_2ZnS_5$. For the $Nd^{3+}$ ions in $BaNd_2CoS_5$, it is considered that the ground-state doublet constitutes the antiferromagnetic state and the first and second excited Kramers' doublets yield the Schottky anomaly at around 60 K in the $C_{mag} - T$ curve from the analogy with the temperature dependence of $C_{mag}$ and $S_{mag}$ for $BaNd_2ZnS_5$. However, it is difficult to estimate the energy levels for the first and second excited doublets, because the Schottky anomaly at around 60 K overlaps with the $\lambda$-type anomaly due to the antiferromagnetic ordering of the $Co^{2+}$ ions. The value of $S_{mag} = 38.2\ J\ mol^{-1}\ K^{-1}$ at 300 K is slightly smaller than $R(2 \ln 6 + \ln 4)$, where $2R \ln 6$ and $R \ln 4$ ($= R \ln(2S+1)$) are attributable to three doublets of the $Nd^{3+}$ ions and the spin state $S = \frac{3}{2}$ of the $Co^{2+}$ ion, respectively.

### 3.3. Crystal and magnetic structures of $BaNd_2CoS_5$

Fig. 6 shows the powder neutron diffraction patterns of $BaNd_2CoS_5$ at 2.3, 10, and 70 K. The Co and Nd ions showed an antiferromagnetic ordering below 58 K

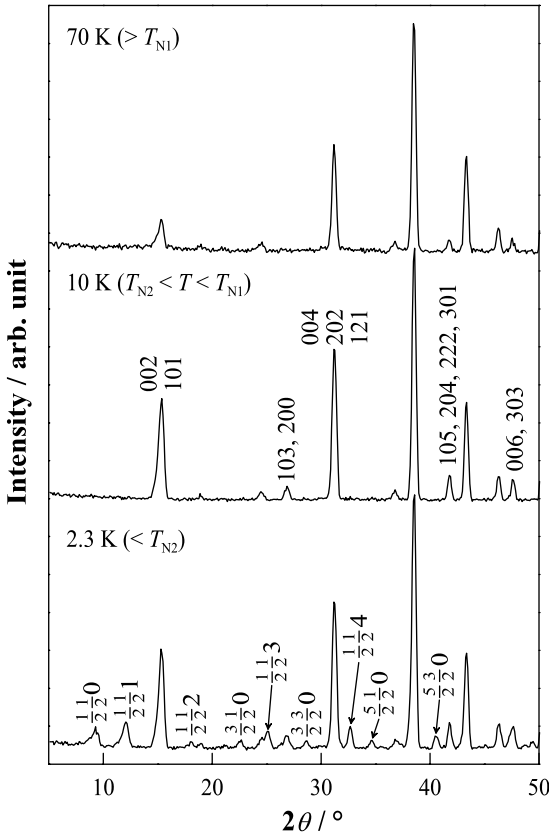


Fig. 6. Powder neutron diffraction patterns for $BaNd_2CoS_5$ at 2.3, 10, and 70 K.

($\equiv T_{N1}$) and 5.7 K ($\equiv T_{N2}$), respectively, through the magnetic susceptibility [12] and the specific heat measurements. Thus, the diffraction pattern at 70 K ($> T_{N1}$) can be indexed on the basis of the chemical cell. The data at 70 K indicate that $BaNd_2CoS_5$ crystallizes in a tetragonal structure with space group of $I4/mcm$ and no structural phase transition occurs between 70 K and room temperature. Table 1 lists the refined lattice parameters and atomic positions of $BaNd_2CoS_5$ at 70 K. The lattice parameters at 70 K refined by the Rietveld analysis are as follows: $a = 7.7816(1)$ Å, $c = 13.5189(4)$ Å (reliability factors of the refinement: $R_{wp} = 11.0\%$, $R_{Bragg} = 4.01\%$).

Table 1
Crystal and magnetic data determined by neutron diffraction at 70 and 10 K for $BaNd_2CoS_5$

| | Site | $x$ | $y$ | $z$ | $B$/Å$^2$ |
|---|---|---|---|---|---|
| 70 K | | | | | |
| Ba | 4*a* | 0 | 0 | 1/4 | 0.01(5) |
| Nd | 8*h* | 0.1624(2) | 0.6624 | 0 | 0.08(3) |
| Co | 4*b* | 0 | 1/2 | 1/4 | 0.54(13) |
| S(1) | 4*c* | 0 | 0 | 0 | 0.54(12) |
| S(2) | 16*l* | 0.1467(3) | 0.6517 | 0.6342(2) | 0.25(1) |
| 10 K | | | | | |
| Ba | 4*a* | 0 | 0 | 1/4 | 0.01(6) |
| Nd | 8*h* | 0.1622(2) | 0.6622 | 0 | 0.07(4) |
| Co | 4*b* | 0 | 1/2 | 1/4 | 0.26(10) |
| S(1) | 4*c* | 0 | 0 | 0 | 0.45(11) |
| S(2) | 16*l* | 0.1470(3) | 0.6470 | 0.6345(2) | 0.30(7) |

Space group: $I4/mcm$
70 K $R_{wp} = 11.0\%$, $R_{Bragg} = 4.01\%$
$a = 7.7816(1)$ Å, $c = 13.5189(4)$ Å
10 K $R_{wp} = 10.6\%$, $R_{Bragg} = 3.60\%$, $R_{mag} = 4.76\%$
$a = 7.7782(1)$ Å, $c = 13.5132(4)$ Å, $m = 3.44(4)\,\mu_B$

*Note*: $R_{wp} = \left[\sum w(y(o)-y(c))^2 / \sum wy(o)^2\right]^{1/2}$, $R_{Bragg} = \sum |I(o) - I(c)| / \sum I(o)$, $R_{mag} = \sum |I_{mag}(o) - I_{mag}(c)| / \sum I_{mag}(o)$.

In the diffraction pattern at 10 K ($T_{N2} < T < T_{N1}$), no additional reflections appear, but magnetic Bragg intensities, which arise from scattering on ordered magnetic moments of the Co ions, are observed for the $\{hkl\}$ reflections with even $h$, $k$, $l$ or with odd $h + k$ and $l$ as compared with the pattern at 70 K. The former reflection condition, which satisfies with a ferromagnetic structure, is excluded for the antiferromagnetic ordering of the $Co^{2+}$ moments. The Co ions occupy the 4*b* site with the following coordinates:

Co(1) $(\frac{1}{2}, 0, \frac{1}{4})$, Co(2) $(\frac{1}{2}, 0, \frac{3}{4})$,
Co(3) $(0, \frac{1}{2}, \frac{1}{4})$, Co(4) $(0, \frac{1}{2}, \frac{3}{4})$.

Then, the collinear antiferromagnetic structure of the $Co^{2+}$ moments has three possible ordering models:

Model I : $m_1 - m_2 + m_3 - m_4$,
Model II : $m_1 + m_2 - m_3 - m_4$,
Model III : $m_1 - m_2 - m_3 + m_4$,

where $m_i$ is the magnetic moment of the Co($i$) ion. Only the magnetic ordering of model III satisfies the $\{hkl\}$ reflection condition with odd $h + k$ and $l$. The Rietveld analysis by using model III determined that the magnetic moment of $Co^{2+}$ was 3.44(4) $\mu_B$ and oriented along the $c$-axis. The best result of the Rietveld fitting is shown in Fig. 7 and the refined crystallographic and magnetic parameters are summarized in Table 1. The schematic magnetic structure is illustrated in Fig. 8. This magnetic ordering is isostructural with that of $BaLa_2CoS_5$ and its magnetic moment agrees with the $Co^{2+}$ moment of 3.53 $\mu_B$ in $BaLa_2CoS_5$ at 10 K [16]. The antiferromagnetic transition temperature (58.1 K) of $Co^{2+}$ for $BaNd_2CoS_5$ was found to be in agreement with that (63.2 K) for $BaLa_2CoS_5$ through the specific heat measurements [16]. From these results, it is inferred that the magnetic interactions between the $Co^{2+}$ and $Nd^{3+}$ moments are extremely weaker than those between the $Co^{2+}$ moments, and that the $Nd^{3+}$

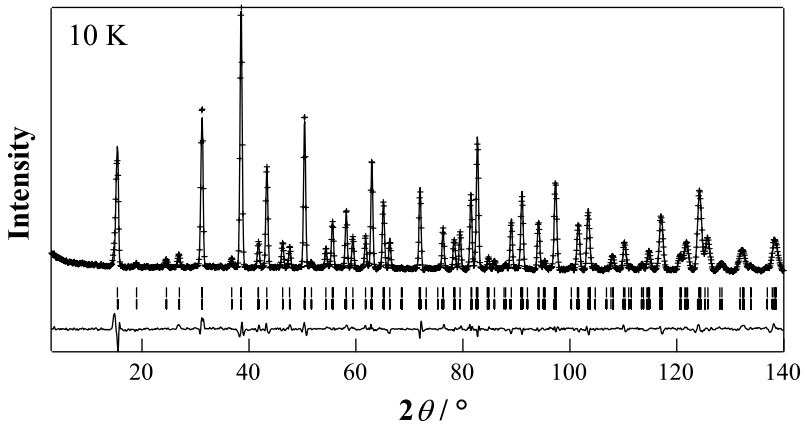


Fig. 7. Powder neutron diffraction pattern and Rietveld refinements for $BaNd_2CoS_5$ at 10 K. The magnitude of magnetic moments is determined to be 3.44(4) $\mu_B$. Reliability factors of the refinement are as follows: $R_{Bragg} = 3.60\%$, $R_{mag} = 4.76\%$.

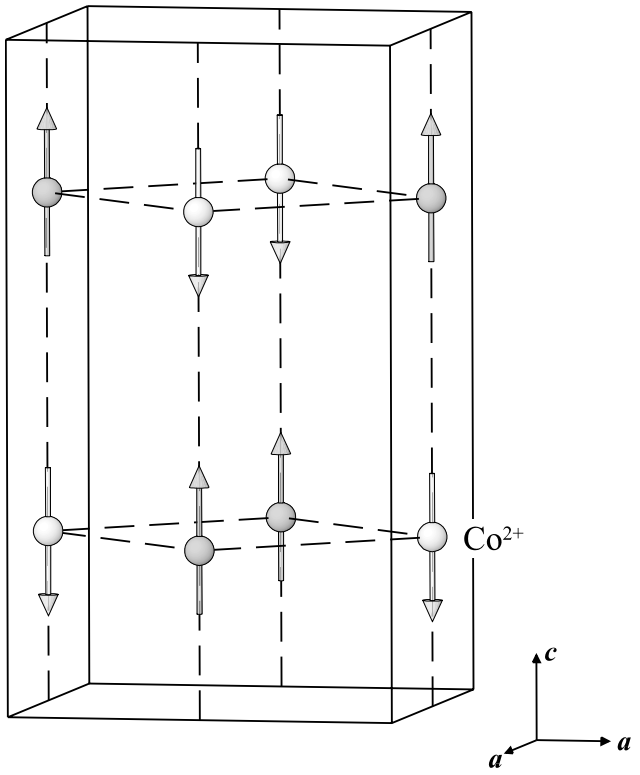


Fig. 8. Orientation of the magnetic moment of $Co^{2+}$ in $BaNd_2CoS_5$ at 10 K.

moments scarcely affect the magnetic orderings of $Co^{2+}$.

In the diffraction pattern at 2.3 K ($< T_{N2}$), additional magnetic peaks, which are due to an antiferromagnetic ordering of the $Nd^{3+}$ moments, are observed for the $\{\frac{hk}{22}l\}$ reflections with odd $h$ and $k$ as compared with the pattern at 10 K. Then, the magnetic unit cell at 2.3 K has a dimension $\sqrt{2}a \times \sqrt{2}a \times c$ in terms of the tetragonal chemical cell. In this unit cell, the $Nd^{3+}$ ions occupy the sites with the following coordinates:

$$\begin{aligned}
&\mathrm{Nd}(1)\ (\tfrac{1}{4},\tfrac{1}{4}+x,0), \quad \mathrm{Nd}(2)\ (\tfrac{1}{4},\tfrac{1}{4}-x,0),\\
&\mathrm{Nd}(3)\ (\tfrac{3}{4}-x,\tfrac{1}{4},0), \quad \mathrm{Nd}(4)\ (\tfrac{3}{4}+x,\tfrac{1}{4},0),\\
&\mathrm{Nd}(5)\ (\tfrac{3}{4},\tfrac{1}{4}+x,\tfrac{1}{2}), \quad \mathrm{Nd}(6)\ (\tfrac{3}{4},\tfrac{1}{4}-x,\tfrac{1}{2}),\\
&\mathrm{Nd}(7)\ (\tfrac{1}{4}-x,\tfrac{1}{4},\tfrac{1}{2}), \quad \mathrm{Nd}(8)\ (\tfrac{1}{4}+x,\tfrac{1}{4},\tfrac{1}{2}),
\end{aligned}$$

where $x$ is identical with a positional parameter $x$ in the $8h$ site, $(x, x-\frac{1}{2}, 0)$, for the chemical cell with the space group, $I4/mcm$. In addition, more eight sites Nd($i$) ($i = 9, 10, \ldots, 16$) were generated by translation of $(\frac{1}{2},\frac{1}{2}, 0)$ for Nd($i$) ($i = 1, 2, \ldots, 8$). The magnetic reflection condition for the $\{\frac{hk}{22}l\}$ reflection with odd $h$ and $k$ leads that the magnetic moment of the Nd($i$) ion is antiparallel to that of the Nd($i+8$) ion. From the magnetic Bragg intensities of the $Nd^{3+}$ moments, it was found that the $Nd^{3+}$ magnetic structure was not a collinear antiferromagnetic structure. Unfortunately, we could not determine the magnetic structure of the $Nd^{3+}$ sublattice, because there are too many sites for the $Nd^{3+}$ ions, 16 sites per magnetic unit cell.

## References

[1] J. Flahaut, P. Laruelle, in: L. Eyring (Ed.), Progress in the Science and Technology of the Rare Earths, Vol. 3, Pergamon Press, Oxford, 1968, pp. 149–208.
[2] J. Flahaut, P. Laruelle, in: L. Eyring (Ed.), Progress in the Science and Technology of the Rare Earths, Vol. 3, Pergamon Press, Oxford, 1968, pp. 209–283.
[3] J. Flahaut, in: K.A. Gschneidner Jr., L.R. Eyring (Eds.), Handbook on the Physics and Chemistry of Rare Earths, Vol. 4, North-Holland Publishing Company, Amsterdam, New York, Oxford, 1979, pp. 1–88.
[4] P.M. van Calcar, P.K. Dorhout, Mater. Sci. Forum 315–317 (1999) 322–330.
[5] W. Ping, J.A. Ibers, J. Solid State Chem. 107 (1993) 347–355.
[6] W. Ping, A.E. Christuk, J.A. Ibers, J. Solid State Chem. 110 (1994) 337–344.
[7] W. Ping, J.A. Ibers, J. Solid State Chem. 110 (1994) 156–161.
[8] R.L. Gitzendanner, C.M. Spencer, F.J. DiSalvo, M.A. Pell, J.A. Ibers, J. Solid State Chem. 131 (1997) 399–404.
[9] P. Stoll, P. Durichen, C. Nather, W. Bensch, Z. Anorg. Allg. Chem. 624 (1998) 1807–1810.
[10] H. Masuda, T. Fujino, N. Sato, K. Yamada, J. Solid State Chem. 146 (1999) 336–343.
[11] M. Wakeshima, Y. Hinatsu, J. Solid State Chem. 153 (2000) 330–335.
[12] M. Wakeshima, Y. Hinatsu, J. Solid State Chem. 159 (2001) 163–169.
[13] K. Ino, M. Wakeshima, Y. Hinatsu, Mater. Res. Bull. 36 (2001) 2207–2213.
[14] M. Wakeshima, K. Ino, Y. Hinatsu,Y. Ishii, Bull. Chem. Soc. Jpn. (2003), in press.
[15] M. Wakeshima, Y. Hinatsu, K. Oikawa, Y. Shimojo, Y. Morii, J. Mater. Chem. 10 (2000) 2183–2185.
[16] M. Wakeshima, Y. Hinatsu, Y. Ishii, Y. Shimojo, Y. Morii, J. Mater. Chem. 12 (2002) 631–634.
[17] K. Ohoyama, T. Kanouchi, K. Nemoto, M. Ohashi, T. Kajitani, Y. Yamaguchi, Jpn. J. Appl. Phys. 37 (1998) 3319–3326.
[18] J. Rodrigues-Carvajal, Physica B 192 (1993) 55–69.
[19] S.J. Joshua, A.P. Cracknell, Phys. Lett. A 28 (1969) 562–563.